Infrared cavity ringdown spectroscopy of water clusters: O–D stretching bands

J. B. Paul, R. A. Provencal, C. Chapo, A. Petterson, and R. J. Saykally
Department of Chemistry, University of California, Berkeley, California 94720

(Received 3 August 1998; accepted 9 September 1998)

The infrared O–D stretching spectrum of fully deuterated jet-cooled water clusters is reported. Sequential red-shifts in the single donor O–D stretches, which characterize the cooperative effects in the hydrogen bond network, were accurately measured for clusters up to $(D_2O)_8$. Detailed comparisons with corresponding data obtained for $(H_2O)_n$ clusters are presented. Additionally, rotational analyses of two D_2O dimer bands are presented. These measurements were made possible by the advent of infrared cavity ringdown laser absorption spectroscopy (IR-CRLAS) using Raman-shifted pulsed dye lasers, which creates many new opportunities for gas phase IR spectroscopy. © *1998 American Institute of Physics.* [S0021-9606(98)00847-2]

I. INTRODUCTION

There is much current interest in the study of gaseous water clusters by modern laser spectroscopy methods,[1–3] as such studies promise a route to an enhanced understanding of the enigmatic condensed phase behavior of water.[4] In addition to vibration-rotation tunneling (VRT) spectra that probe cluster structures and intermolecular force fields,[1] measurements of the stretching and bending vibrations of the chemical (O–H) bonds are crucial because these directly probe the cooperativity in the hydrogen bond network and the geometric distortion of the water monomer that accompanies H-bond formation. Moreover, it is important to obtain data for several isotopomers, as these provide exacting constraints on the force field determination. Previous gas phase IR measurements[5–9] have been restricted to the O–H stretch region (2.6–3.0 μm) because of the lack of suitable light sources to extend the frequency coverage to other regions. Here we report the application of the novel and more general cavity ringdown laser absorption spectroscopy (CRLAS) technique for the first measurement of the O–D stretch vibrations in jet-cooled $(D_2O)_n$ clusters, which provides new insight into the nature of water cluster vibrations. The spectrometer used in this study operates continuously in the 2.5–7 μm spectral region, with an average fractional absorption sensitivity of 1–2 ppm.

Water cluster O–H stretch fundamentals were first observed in the gas phase by Lee and co-workers,[6] using an approach based on vibrationally predissociating the weakly bound clusters with a pulsed, tunable OPO laser operating in the 3 μm region. Limitations in nonlinear crystal technology that continue to exist today prevent these lasers from generating usable power at wavelengths longer than 4.0 μm, thus precluding studies of the corresponding stretching bands in D_2O clusters. Subsequently, many other gas phase studies of water clusters have been reported.[5,8,10,11] Other studies of water clusters include matrix isolation experiments[12,13] and theoretical[14,15] calculations.

Studies of fully deuterated water clusters in the O–D stretching region are now made possible by the advent of the IR-CRLAS method, which has been described previously.[16,17] For the dimer, this has already produced an improved understanding of the ground and excited state acceptor tunneling dynamics of the acceptor anti-symmetric stretch.[16] In the present work, we have recorded the discrete absorption bands of $(D_2O)_n$ clusters ($n<9$), including a detailed analysis of two additional dimer bands, which are complicated by the numerous tunneling effects and are only partially rotationally resolved. Additionally, a continuum absorption associated with clusters ranging in size from hundreds to thousands of water molecules per cluster is discussed. These new results are compared with those for H_2O clusters in the gas phase, and D_2O clusters in rare-gas matrices.

II. EXPERIMENT

The IR-CRLAS apparatus used to conduct these experiments has been discussed previously.[16,18] Briefly, tunable infrared radiation is generated by Raman shifting a pulsed dye laser (Lambda Physik f13002e) into the third-Stokes band using a multi-pass cell containing 200 p.s.i. of H_2 gas. The bandwidth of the dye laser was switchable from 0.2 to 0.04 cm^{-1} by installing an intracavity etalon. After spectral filtering, the laser light is aligned into a two mirror Ringdown cavity. The light leaving the cavity is focused by a 10 cm lens onto an LN_2-cooled InSb detector. The resultant signal is amplified, digitized, and transferred to a PC for real-time fitting to an exponential decay. The determined time constant is divided into the cavity optical transit time to yield the per pass fractional cavity intensity loss.

The water clusters were generated in a pulsed supersonic expansion. The helium carrier gas was bubbled through a reservoir of room temperature water, and directed into a 4 in. slit source[19] contained within a Roots pumped vacuum chamber. Various methods were used to systematically adjust the expansion conditions, including altering the source stagnation pressure and limiting the amount of water in the expansion with a needle valve, as discussed below.

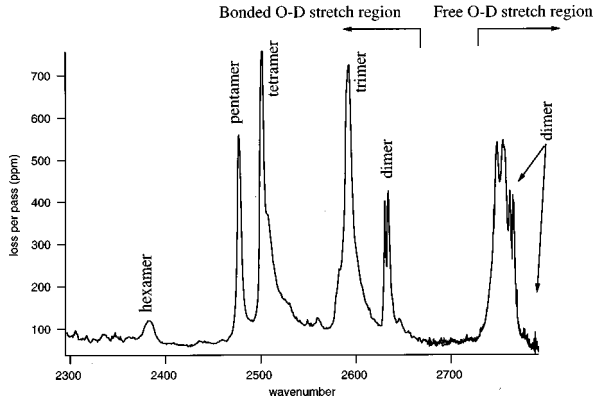

FIG. 1. The O–D stretching spectrum of fully deuterated water clusters taken under expansion conditions favoring the formation of small clusters ($n<10$) but with a high degree of internal cooling (see text for details). From *ab initio* integrated absorption cross sections (Ref. 22), we estimate the density of trimers and tetramers in the expansion ($\sim$1 cm from the orifice) to be $3\times10^{13}/\mathrm{cm}^3$, and $7\times10^{12}/\mathrm{cm}^3$, respectively.

III. RESULTS

Figure 1 shows a survey scan of the entire O–D stretching spectral region, with the band locations and most probable spectral assignments given in Table I. As expected, the spectrum resembles the O–H stretching spectrum observed for H_2O clusters under similar conditions. As such, many of the features can be assigned by inspection. The bands separate into characteristic absorptions regions, wherein the ''free'' O–D stretches are tightly grouped around 2700 cm^{-1}, while the ''bonded'' stretches exhibit large red-shifts, extending hundreds of wave numbers toward lower frequency. These red-shifts are a direct measure of the cooperative effects within the hydrogen-bond network.

The least red-shifted of the bonded stretches belongs to the dimer. While H_2O dimer stretch was found to be severely lifetime broadened,[11,18] the D_2O cluster shows well-resolved rotational structure of a parallel transition, permitting a detailed analysis. This band system, occurring at 2632 cm^{-1} (Fig. 3.2), is the most intense of the observed $(D_2O)_2$ bands. Two main progressions can be identified, despite the significant spectral congestion caused by the tunneling splittings and the parallel band structure. A close inspection reveals that the weaker progression lacks transitions involving the $J''=0$ state, possesses a Q-branch, and exhibits a splitting in the high-J rotational lines, indicating that it results from a $K_a=1\leftarrow1$ transition of a nearly symmetric rotor. Therefore, we assign both of these progressions to the A_1 symmetry component of the acceptor switching doublet. With this assignment, these progressions were fit to a standard energy level expression to derive molecular constants for the vibrationally excited state. A simulation based on these constants is also shown in Fig. 2, while the generated constants are listed in Table II.

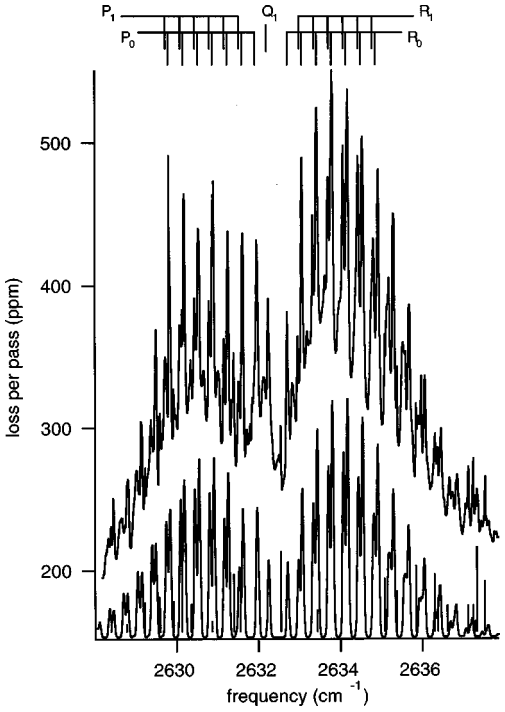

FIG. 2. IR-CRLAS spectrum of the $(D_2O)_2$-bonded O–D stretch. Below is a simulation based on the molecular constants listed in Table II and a rotational temperature of 10 K. The sticks represent D_2O monomer transitions, which were used to frequency calibrate the data.

TABLE I. Measured band positions and assignments for $(D_2O)_n$ clusters.

Frequency (cm^{-1})	Shift (cm^{-1})[a]	Assignment	Description (O–D stretch)
2783.14	−6	dimer	acceptor antisymmetric
2765	−24	dimer	donor free
2756	−33	trimer	free
2749	−40	tetramer/pentamer	free
~2743	−46	>pentamer	free
2640	−149	>hexamer	double-donor?
2632	−157	dimer	donor bonded
2592	−197	trimer	bonded
2588	−201	trimer	shoulder
2570	−219	>hexamer	double-donor?
2506	−283	tetramer	shoulder
2501	−288	tetramer	bonded
2477	−312	pentamer	bonded
2450	−339	>hexamer	?
2395	−394	hexamer	single-donor
2340	−449	octamer	single-donor

[a]Shift relative to D_2O monomer anti-symmetric stretch (2789 cm^{-1}).

TABLE II. Determine molecular constants of the $(D_2O)_2$ bonded and free O–H stretches. All constants given in cm^{-1}.

Constant\band	Bonded O–H	Free O–H
Band origin (ν_0)	2632.33(1)	2763.39(1)
ΔA	−0.10(1)	−0.19(1)
$K_a'=0$		
$(B+C)/2'$	0.182 02(2)	0.181 48(12)
D'	0*	0.000 002 5(10)
$K_a'=1$		
$(B+C)/2'$	0.181 77(2)	0.181 40(14)
D'	0*	0.000 004 5(10)
$(B-C)'$	0.0036(1)	-

*Fixed.

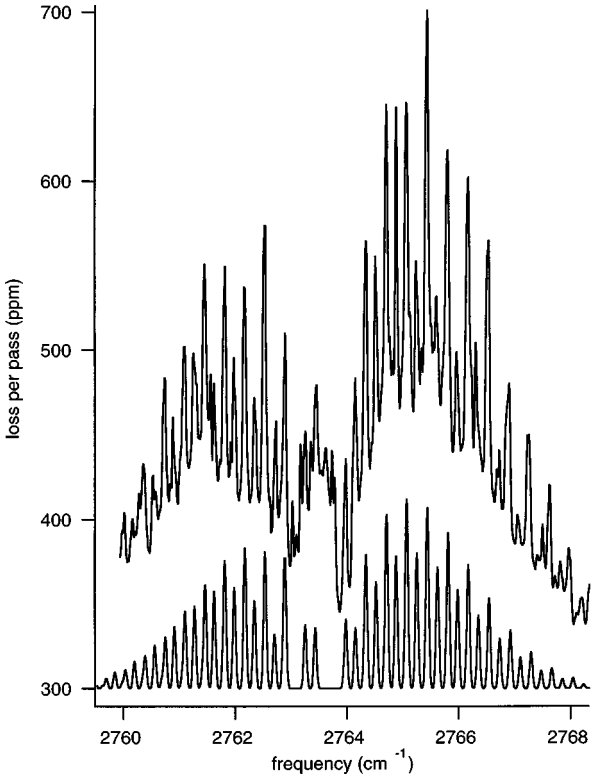

FIG. 3. The donor free O–D stretch of $(D_2O)_2$, measured by IR-CRLAS, and simulation based on the constants in Table II.

A third, even weaker progression can also be identified within this band system, which presumably corresponds to the other acceptor switching component (A_2 symmetry). This tunneling motion, which is the only one of the three presently accepted feasible tunneling pathways that does not require breaking a hydrogen bond, is also the only one that commonly produces large enough splittings to be resolved at the present resolution. Assuming that the splittings from the other two tunneling motions (donor–acceptor interchange and bifurcation) are unresolved, the intensity ratio of the acceptor tunneling components is expected to be 2:1 based on nuclear spin statistics, which agrees well with the present results. Unfortunately, this progression is too weak to permit rotational analysis.

The donor free stretch, measured near 2765 cm^{-1}, exhibits structure similar to the bonded stretch (Fig. 3), aside from the lack of observable subbands belonging to the A_2 states. We assume that these exist, but in this case are coincidentally beneath rather than in between the A_1 transitions. Accordingly, we have analyzed this band in the same manner as the bonded stretch by assigning all of the strong lines to A_1 symmetry. The fitted constants are given in Table II.

In Fig. 4, IR-CRLAS spectra of H_2O [Fig. 4(a)] and D_2O [Fig. 4(b)] clusters are directly compared, while the ratios of the frequencies of the H_2O bands to those of the corresponding D_2O bands are plotted in Fig. 4(d) as a function of cluster size. The monotonic shape of this plot indicates that all of these bands arise from single-donor stretching vibrations, which are predicted to show increasing red-shifts with increasing cluster size. This shift depends on both the vibrational reduced mass and the force constant ($\omega \propto \sqrt{k/\mu}$), however, the ratio of these shifts among isotopomers should depend primarily on the reduced masses, as the anharmonicity is expected to be small for these high frequency vibrations. Therefore, because $\omega_{OH}/\omega_{OD} \approx \sqrt{\mu_{OD}/\mu_{OH}}$, the trend in Fig. 4(d) can be interpreted as an increasing heavy atom involvement in the vibrations of larger clusters due to increased delocalization of the vibrational motion, as predicted by theory.[20]

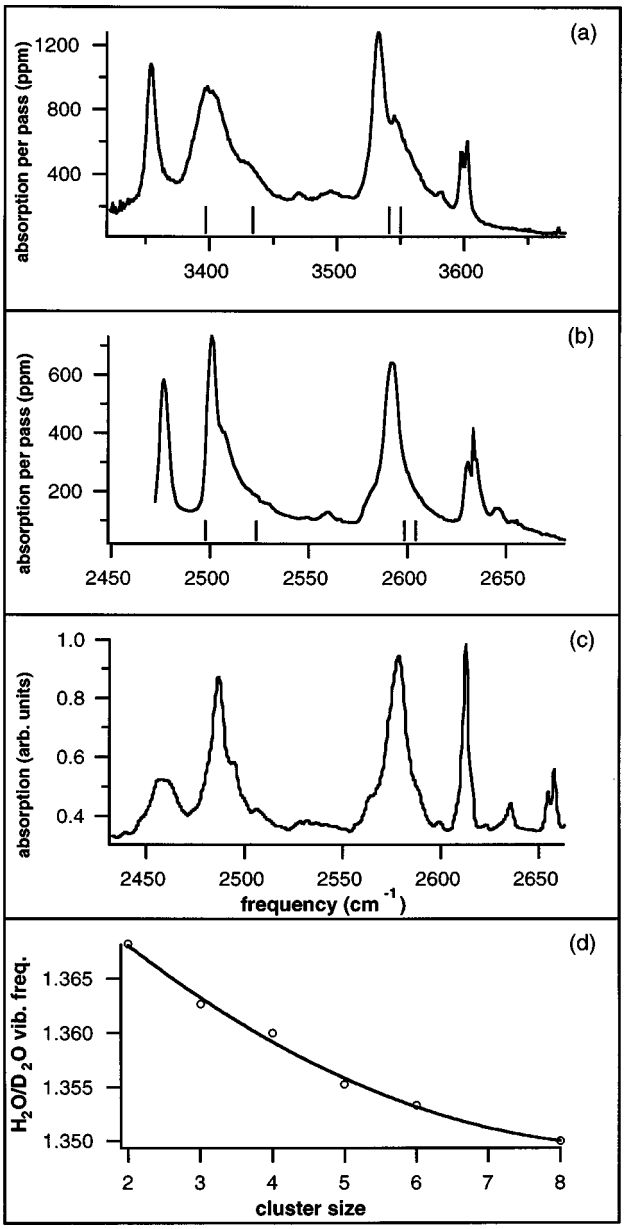

FIG. 4. Comparison of H_2O and D_2O cluster absorption spectra and *ab initio* estimates. (a) IR-CRLAS H_2O cluster spectra. Sticks represent the *ab initio* predictions for $(H_2O)_3$ and $(H_2O)_4$ from Ref. 14. These values, when scaled by 0.975 (as shown), agree quite well with the measured band positions. (b) D_2O cluster data obtained under similar conditions as in (a). In this case, the *ab initio* values (Ref. 22) are scaled by 0.98, but the agreement with the experimental results is somewhat poorer than in (a). (c) D_2O clusters in an argon matrix at 7 K (Ref. 13). Note the frequency scale is the same as in (b), although shifted by 17 cm^{-1}. (d) Plot of the ratio of vibrational frequencies of the corresponding single-donor stretches in H_2O and D_2O clusters vs cluster size. This trend reflects the increasing heavy atom involvement in the vibrational motion for the larger clusters.

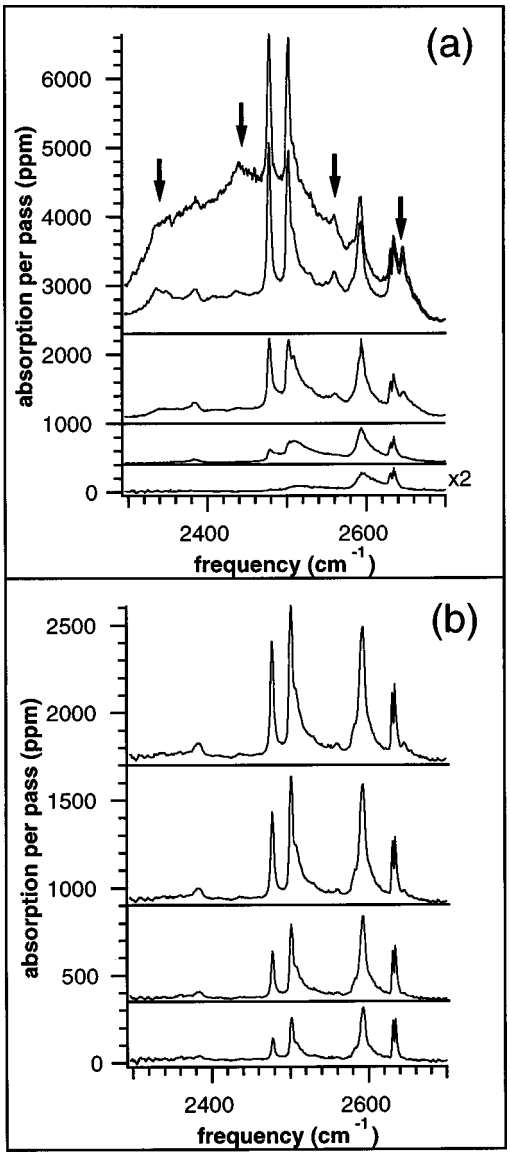

FIG. 5. (a) D_2O cluster spectra as a function of source pressure. Scans are taken at 10, 15, 25, 35, and 45 p.s.i. absolute pressure. Note to two uppermost pressure scans are plotted with the same offset to highlight the ''bulk ice'' feature that appears for the highest source pressure. (b) D_2O cluster spectra obtained with a constant source pressure (35 psia) and increasing concentration of water in the carrier gas.

To more effectively discriminate the band shapes and spectral carriers of the various absorption features, two slightly different cluster source configurations were employed. First, we employed the ''standard'' configuration of bubbling the helium carrier gas through a 25 °C water reservoir, saturating it with water vapor, and routing it directly to the pulsed slit jet. The water cluster spectra were then recorded [Fig. 5(a)] as a function of carrier gas pressure (measured before the bubbler). With backing pressures below 1 atm, only small clusters are observed,[18] and apparently only with a moderate degree of internal cooling (see below). As the source backing pressure is raised, the characteristic rotational and vibrational temperatures decrease. This is manifested as a narrowing of the band shapes, causing the more closely spaced features to become resolved. The colder expansions also naturally increase the degree of clustering. This, combined with the relatively high absolute concentration of water in the expansion ($\sim$1%), results in the production of very large clusters at source backing pressures exceeding 3 atm. In fact, the IR spectrum of these ice ''nanoparticles'' resembles that of amorphous ice,[18] a highly disordered bulk phase that forms when water vapor deposits slowly on a cryogenic (4–100 K) substrate.

In the second configuration, the water/He mixture was slightly overpressurized, and admitted into a primary carrier gas flow through a needle valve. This was done to finely regulate the water concentration in the resulting mixture, without changing the total stagnation pressure. With this approach, a relatively constant expansion temperature is maintained as the water concentration is adjusted. The band shapes are observed to remain constant using this procedure due to the approximately constant beam temperature [Fig. 5(b)], which allows the variations of the band intensities with respect to changes in water concentration to be recorded more accurately. This reproducible control over the relative concentrations of the individual clusters aids in carrier identification through comparison of the relative growth rates of the individual features. Techniques similar to this have been used extensively in matrix isolation spectroscopy to determine spectral carriers, viz. varying the deposition concentration or annealing the matrix.[13,21] Additionally, by limiting the total amount of water vapor in the carrier gas, a more accurate characterization of the individual band shapes at very low temperatures can be obtained without the interference of the much larger ''ice like'' clusters that would otherwise result at higher backing pressures.

IV. DISCUSSION

A. D_2O dimer

In Fig. 6, the corresponding H_2O and D_2O dimer bonded stretches, as measured by CRLAS, are shown for comparison. The severe lifetime broadening apparent in the H_2O band is noticeably absent in D_2O. The increased reduced mass, reduced excitation energy, and higher binding energy in the D_2O form of the dimer apparently allow for a significantly longer predissociation lifetime. However, a close inspection of individual lines in the D_2O case reveals that lifetime broadening still contributes to the measured lineshape, producing smooth line shapes with no traces of substructure. This structure, which is observed in the corresponding acceptor anti-symmetric stretch, is expected from the triplet splitting caused by donor–acceptor interchange tunneling. Therefore, we can use the measured linewidths to estimate the excited-state lifetime for both isotopomers. For H_2O, this results in a lifetime of 80 ps (0.2 cm^{-1}), while for D_2O the lifetime increases from this by a factor of 40 to about 5 ns. Characterizing the relative predissociation dynamics in $(H_2O)_2$ and $(D_2O)_2$ in detail would be a most interesting theoretical project.

As was the case for H_2O clusters, we have not observed the acceptor symmetric stretch. Studies of water clusters in cryogenic matrices show that the symmetric stretch absorption intensity is substantially weaker (by about a factor of 10) than that of the anti-symmetric stretch.[13,21] Considering

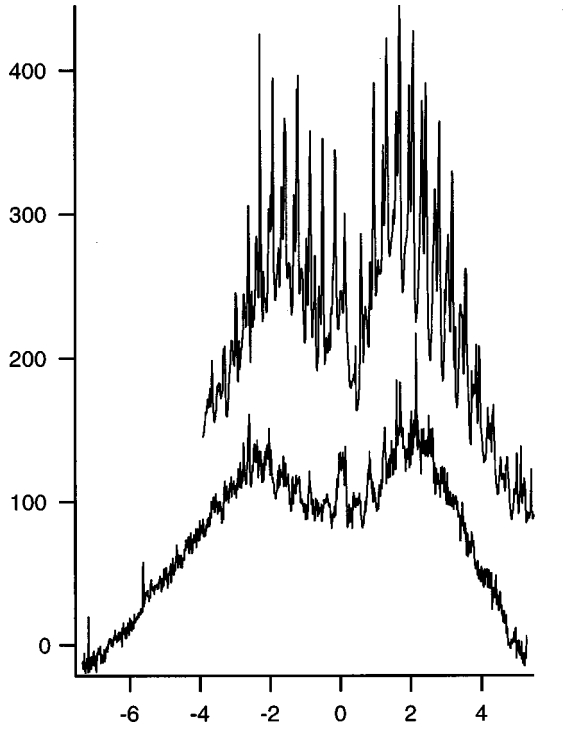

FIG. 6. Comparison of the corresponding dimer bonded stretches (D_2O, upper; H_2O, lower) highlighting the rapid predissociation in $(H_2O)_2$. By comparing linewidths, we estimate a factor of 40 reduction in the upper state lifetime of $(H_2O)_2$ compared with $(D_2O)_2$.

the signal-to-noise with which we observe the antisymmetric stretch,[16] this reduction in intensity is sufficiently large to explain its absence in the spectrum. Nevertheless, the matrix results can be used to gain a good understanding of where the band is likely to be located in the gas phase. The presence of the matrix induces a remarkably uniform red-shift of 17 cm^{-1} from the corresponding the gas phase frequencies, regardless of cluster size (Fig. 4). This locates the missing gas phase band near 2680 cm^{-1}.

B. Cyclic clusters: $n=3-5$

A close inspection of the absorption bands of the small cyclic clusters generated at low expansion temperatures reveals a number of subtle features. Most notably, both the trimer and tetramer peaks show partially resolved shoulders. In both cases, the variation of this structure with changes in water concentration [Fig. 5(b)] indicates that these belong to the same cluster as the adjacent dominant peak. For the trimer, the shoulder appears at lower frequency relative to the main peak. While a very similar feature is also clearly observed in matrix isolation studies [Fig. 4(b)] *ab initio* MP2 calculations(20)[22] predict two IR active bands separated by 6 cm^{-1}, with the weaker band (by ~8%) at higher energy.

This is interesting because $(H_2O)_3$ exhibits a partially resolved blue-shifted feature [Fig. 4(a)], which is in better agreement with theory.[14] Both features in H_2O spectrum were established as trimer bands by the recent work of Huisken and co-workers, wherein gaseous free water clusters[8] and water clusters embedded in large liquid helium clusters[23] were examined. They observe a 13 cm^{-1} splitting for $(H_2O)_3$ embedded in helium ''nanomatrices,'' while the gaseous cluster band showed a significant broadening that shaded toward higher frequency. We find a splitting of 11 cm^{-1}, which agrees well with the previous results, including MP2 calculations,[14] which predict two IR-active bands split by 9 cm^{-1}, with a third, primarily Raman-active transition red-shifted by an additional 60 cm^{-1}. However, theory predicts the two IR-active modes should have roughly equal intensity. This agrees only marginally with the experimental results, which exhibit a 3:1 intensity ratio between the features.

Concerning the assignment of the partially resolved feature on the high frequency side of the main $(D_2O)_4$ peak, the results of our growth-rate studies mentioned above are supported by the following arguments. Matrix isolation studies show a similar feature, which was tentatively assigned to the tetramer.[13] Additionally, the most intense vibrational modes of clusters larger than the pentamer are predicted to be the single-donor stretches,[15] which should be found at lower frequencies than the 2477 cm^{-1} $(D_2O)_5$ band. Since the feature in question appears stronger than any found in this region, the likelihood of the carrier being larger than the pentamer is small. However, as for the trimer, *ab initio* calculations apparently overestimate the splitting between these bands,[22] predicting two IR-active modes (a strong degenerate mode and a much weaker, nondegenerate mode) separated by 25 cm^{-1}, which should be compared with the ~4 cm^{-1} splitting presently observed. For $(H_2O)_4$, our observed splitting is ~26 cm^{-1}, which agrees somewhat better with the predicted value of 38 cm^{-1}.[14] Again, the agreement between the predicted and measured relative band intensities of these modes is poor: a 200:1 intensity ratio is predicted, while we observe 3:1.

In contrast with the smaller cyclic clusters, both $(H_2O)_5$ and $(D_20)_5$ absorptions appear as single narrow peaks (at low temperature). While the reasons for this are not obvious, there exists at least one notable difference between the pentamer and the smaller ring clusters, which is that the puckered-ring oxygen framework of the pentamer is considerably ''floppier'' than the planar rings of the smaller clusters. Therefore, the coupling between the intra- and intermolecular vibrational modes is probably considerably stronger than in the trimer or tetramer.

Finally, it is easily seen in Fig. 5(a) that at higher expansion temperatures (lower stagnation pressures) the absorption profiles extend 50–100 cm^{-1} from the sharp bandhead like features toward higher frequency. These profiles sharpen as the source stagnation pressure is raised causing the expansion temperature to decrease. Because the energy spreads exhibited in these spectra are far too large to be explained by a single rovibrational manifold, the most likely explanation for this behavior is that the low-lying intermolecular vibrational modes (20–100 cm^{-1}) are being thermally populated at low stagnation pressures. For this to be the case, the frequencies of these modes must be increasing in the O–D stretching excited state to explain the shading toward higher frequency.

C. Larger clusters: $n>5$

The absorption feature at 2395 cm^{-1} is analogous to a band assigned to the hexamer in the H_2O cluster spectrum at 3220 cm^{-1}.[18] This appears to be the appropriate assignment in the present case as well. *Ab initio* calculations indicate that bands with such large red-shifts should appear for single-donor chromophores in clusters containing double hydrogen bond-donating monomers, while the double-donor stretches themselves are predicted to absorb more weakly in the 2500–2600 cm^{-1} region.[15] As terahertz laser VRT spectroscopy studies indicate that the hexamer is the smallest cluster to contain double donors,[2] and since this feature is the first to appear in this region as the expansion conditions are altered to increase clustering, we are confident that this band is indeed due to the hexamer.

Several other discrete absorption features also apparently belong to small nonplanar clusters that are larger than the pentamer. The most notable are found at 2640 cm^{-1}, 2570 cm^{-1}, 2450 cm^{-1}, and 2340 cm^{-1} [marked by arrows in Fig. 5(a)]. These features develop subsequently to the hexamer band as the source stagnation pressure is raised, and eventually become considerably larger than their respective maximum intensities in Fig. 5b, wherein the amount of water in the expansion was limited. This behavior is clearly unlike the smaller cluster bands ($n<6$). However, the discrete nature of these absorptions indicates that the responsible clusters are either fairly small ($n<20$) or highly symmetric, or both.

The 2340 cm^{-1} absorption probably corresponds to the cubic octamer, continuing the trend of sequential red-shifts of single-donor chromophores with increasing cluster size. This band is analogous to the 3180 cm^{-1} feature found in the H_2O cluster spectrum. The recent benzene-$(H_2O)_8$ study of Gruenloh *et al.*[3] provides strong support for this assignment, as three bands centered around 3150 cm^{-1} were observed in their study. The 2640 cm^{-1} absorption is interesting because it is the only prominent feature to occur blue-shifted relative to the dimer bonded stretch. While *ab initio* studies of the octamer show bands with significant absorption intensity in this region,[15] still larger clusters, and possibly the hexamer and heptamer as well, could also have bands in this region. It is not possible to definitively assign this feature at this time, however, we can at least assume that the responsible cluster is larger than the pentamer, as the cyclic clusters are highly unlikely to have strong bands in this region. Interestingly, the most likely H_2O analog of this feature is the weak absorption at 3580 cm^{-1}, which is *not* blue-shifted relative to the dimer. Concerning the two remaining features, which are possibly double-donor stretching bands, not much else can be said aside from the assignment to the size range given above. Clearly, high level *ab initio* calculations on these larger water clusters would be most useful.

As the pressure is further increased, a very broad continuum absorption centered around 2500 cm^{-1} and extending between 2700 and 2200 cm^{-1} becomes apparent, which is analogous to the ''liquidlike'' feature discussed previously for the case of H_2O clusters.[18] The clusters contributing to this feature are estimated to be in the $n=20-100$ range. At still higher pressures, a broad ''icelike'' absorption due to very large clusters ($n>100$) becomes significant. As expected with the transition from medium to the large sized clusters, the spectrum narrows (to $\sim$200 cm^{-1} FWHM) and shifts to the red (by $\sim$50 cm^{-1}). The narrowing reflects the increasing order in the larger clusters as the contributions from the ''edges'' of the cluster become less significant, while the red-shift arises from that fact that the vibrations are delocalized throughout the cluster, and will therefore experience less ''quantum confinement'' as the clusters grow larger. The appearance of this ice feature occurs quite suddenly as the pressure is raised, growing by a factor of at least 3 in the final pressure increment in Fig. 5a. This suggests that a transition point is reached when clusters large enough to act as nucleation sites are produced.

ACKNOWLEDGMENTS

This work was supported by the Chemical Physics Program of the Air Force Office of Scientific Research, and by the Physical Chemistry Division of the National Science Foundation.

[1] K. Liu, J. D. Cruzan, and R. J. Saykally, Science **271**, 929 (1996).
[2] K. Liu, M. G. Brown, C. Carter, R. J. Saykally, J. K. Gregory, and D. C. Clary, Nature (London) **381**, 501 (1996).
[3] C. Gruenloh, J. Carney, C. Arrington, T. S. Zwier, S. Y. Fredericks, and K. D. Jordan, Science **276**, 1678 (1997).
[4] O. Mishima, Nature (London) **392**, 109 (1998).
[5] D. F. Coker, R. E. Miller, and R. O. Watts, J. Chem. Phys. **82**, 3554 (1985).
[6] M. F. Vernon, D. J. Krajnovich, H. S. Kwok, J. M. Lisy, Y. R. Shen, and Y. T. Lee, J. Chem. Phys. **77**, 47 (1982).
[7] R. H. Page, J. G. Frey, Y. R. Shen, and Y. T. Lee, Chem. Phys. Lett. **106**, 373 (1984).
[8] F. Huisken, M. Kaloudis, and A. Kulcke, J. Chem. Phys. **104**, 17 (1996).
[9] R. N. Pribble and T. S. Zwier, Science **265**, 75 (1994).
[10] S. Wuelfert, D. Herren, and S. Leutwyler, J. Chem. Phys. **86**, 3751 (1987).
[11] Z. S. Huang and R. E. Miller, J. Chem. Phys. **91**, 6613 (1989).
[12] A. Engdahl and B. Nielander, J. Chem. Phys. **86**, 4831 (1987).
[13] G. P. Ayers and A. D. E. Pullin, Spectrochim. Acta **32A**, 1629 (1976).
[14] S. S. Xantheas and T. H. Dunning Jr., J. Chem. Phys. **99**, 8774 (1993).
[15] R. Knochenmuss and S. Leutwyler, J. Chem. Phys. **96**, 5233 (1992).
[16] J. B. Paul, R. A. Provencal, and R. J. Saykally, J. Phys. Chem. **102**, 3279 (1998).
[17] J. J. Scherer, J. B. Paul, A. O'Keefe, and R. J. Saykally, Chem. Rev. **97**, 25 (1997).
[18] J. B. Paul, C. P. Collier, J. J. Scherer, A. O'Keefe, and R. J. Saykally, J. Phys. Chem. **101**, 5211 (1997).
[19] K. Liu, R. S. Fellers, M. R. Viant, R. P. McLaughlin, M. G. Brown, and R. J. Saykally, Rev. Sci. Instrum. **67**, 410 (1996).
[20] E. Honegger and S. Leutwyler, J. Chem. Phys. **88**, 2582 (1988).
[21] R. M. Brentwood, A. J. Barnes, and W. J. Orville-Thomas, J. Mol. Spectrosc. **84**, 391 (1980).
[22] M. Schuetz, W. Klopper, S. Graf, and S. Leutwyler (to be published).
[23] R. Fröchtenicht, M. Kaloudis, M. Koch, and F. Huisken, J. Chem. Phys. **105**, 6128 (1996).